Simplified Modeling of Ring Resonator (RR) and Thin Wire Using Magnetization and Polarization with Loss Analysis

Dongho Jeon, Bomson Lee
Dept. Electronics and Radio Engineering, Kyung Hee University
Yongin-si, Gyeonggi-do, Republic of Korea
bomson@khu.ac.kr

Abstract — In this work, the ring resonator (RR) and thin wire are simply modeled using the concept of magnetization and polarization, respectively, with convenient expressions for its effective permeability and permittivity. Equivalent circuits for them are also provided with closed-form expressions for all circuit elements. The ring resonator and the thin wire were designed and their characteristics were examined in terms of S-parameters, effective permeability and permittivity, loss rate, bandwidth, etc. The theoretical, circuit-, and EM-simulated results are shown to be in an excellent agreement. Based on this modeling, loss analysis has been carried out.

I. INTRODUCTION

The realization of media having negative permittivity and permeability, so called left-handed media (or metamaterials), became feasible after 1991 when Pendry proposed to use an array of thin wires and split ring resonators (SRRs) [1-2]. A number of approaches followed in many aspects in an effort to realize similar left-handed characteristics [3-6]. However, most of them have been known to suffer from high losses and narrow bandwidth. Even alleviating these problems could have a significant impact on many applications.

In this paper, we model the ring resonator (the original form of SRRs) excited by a magnetic field as an induced magnetic dipole and derive the effective permeability in a very convenient form. The mechanism of SRRs is explained with more familiar terms than in [1-2]. In addition, we model the thin wire excited by an electric field and the effective permittivity is derived using the similar procedure as used in the RR case. For both the ring resonator and the thin wire, we perform a loss analysis with some examples with respect to the size of unit cell and the radius of each structure. The medium having low loss can be achieved through the modification of geometry based on the loss analysis. The effects of employing these methods are discussed with some comparisons.

II. MODELING OF RING RESONATOR

We model the ring resonator using magnetization concept and provide an equivalent circuit. The ring resonator is shown with the orientations of incident fields in Fig. 1. The TEM wave travels in the z direction with the electric and magnetic fields oriented in the x and y direction, respectively. The radius of the loop is r and the radius of the ring is r_{ring}. The side length of the unit cell is a. C is the capacitance of a chip capacitor loaded on the RR. It is inserted for resonance of the ring resonator at s design angular frequency ω_0. The total resistance R of the ring resonator is given by

$$R = R_r + R_l \tag{1}$$

where R_r is the radiation resistance, R_l is the ohmic resistance. As the magnetic field H_0 couples through the ring resonator, an induced voltage V_{emf} is given by

$$v_{emf} = \frac{\partial\left(\mu_0 H_0 \pi r^2\right)}{\partial t} \xrightarrow{\frac{\partial}{\partial t} = j\omega} V_{emf} = j\omega\mu_0 H_0 \pi r^2 \tag{2}$$

based on Faraday's law.

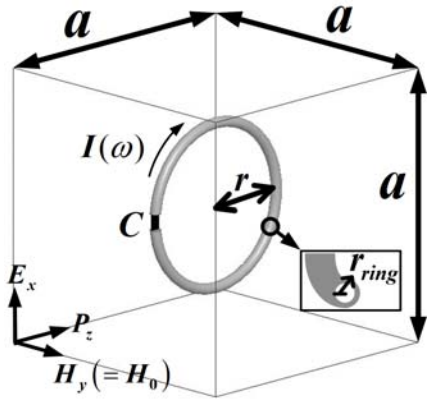

Fig.1. Structure of a ring resonator

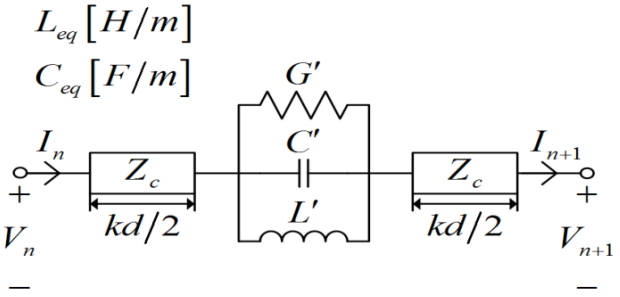

Fig.2. Equivalent circuit of ring resonator

Accordingly, the current I can be determined simply by dividing V_{emf} with the resonator impedance $Z(\omega)$ (series sum of R, L, and C). Using the magnetization defined by $\overline{M}(\omega)=\overline{m}(\omega)/a^3$, the relative effective permeability can be obtained as

$$\mu_{eff}(\omega)=1+\chi_m(\omega)=1-\frac{j\omega\mu_0\left(\pi r^2\right)^2}{a^3R\left[1+jQ\left(\frac{\omega}{\omega_0}-\frac{\omega_0}{\omega}\right)\right]} \tag{3}$$

where ω is the angular frequency, $\overline{m}(\omega)$ is the magnetic dipole moment ($\overline{m}=-I(\omega)\pi r^2\overline{a_y}$), Q ($Q = \omega_0 L/R$) is the quality factor, χ_m is the magnetic susceptibility, and μ_0 is the permeability in free space. Now, we want to devise an equivalent circuit for the structure shown in Fig. 1. By multiplying the derived relative effective permeability with the geometrical factor (g) which is determined for the cross-sectional shape of a specific transmission line, we can obtain the effective inductance of the transmission line given by

$$L_{eff}(\omega)=\mu_0\mu_{eff}(\omega)g\ [H/m]\ . \tag{4}$$

For an instance, g for the parallel plate waveguide T/L with width W and height h is given by h/W. Now, the effective series impedance can be expressed as

$$\begin{aligned} Z(\omega) &= j\omega L_{eff}(\omega)d \\ &= j\omega\mu_0 gd+\frac{1}{\frac{a^3}{\left(\omega\mu_0\pi r^2\right)^2 gd}\left[R+j\omega_0 L\left(\frac{\omega}{\omega_0}-\frac{\omega_0}{\omega}\right)\right]}\ [\Omega] \end{aligned} \tag{5}$$

where d is the physical length of the T/L unit cell. A close examination of (5) leads to the equivalent circuit as depicted in Fig. 2. The equivalent circuit consists of a right handed (RH) transmission line with $L_{eq}d$, $C_{eq}d$ and a parallel G', C', L' resonator in the series branch. The RH T/L may be alternatively represented by Z_c and kd at ω_0. The total series impedance of the equivalent circuit in Fig. 2 can be written as

$$Z_{eq}(\omega)=j\omega L_{eq}d+\frac{1}{G'+j\omega_0 C'\left(\frac{\omega}{\omega_0}-\frac{\omega_0}{\omega}\right)}\ [\Omega] \tag{6}.$$

The value of parameters G', C', L' in (6) can be obtained as (7) by comparing (5) and (6).

$$G'=\frac{a^3}{\left(\omega\mu_0\pi r^2\right)gd}R, C'=\frac{a^3}{\left(\omega\mu_0\pi r^2\right)gd}L, L'=\frac{1}{\omega_0^2 C} \tag{7}$$

III. MODELING OF THIN WIRE

The same manner used in modelling of the ring resonator is employed for the case of thin wire and its equivalent circuit. The structure and dimensions of the thin wire are depicted in Fig. 3. The radius of the wire is r' and the height is same as the one side length of the unit cell a'. Since the total electric field on the surface of the wire should be 0, the induced electric field is $-E_0\overline{a_x}$ as shown in Fig. 3. With the current determined by $I = E_0 a/(R+j\omega L)$, the induced charge on the top of the thin wire is given by $q = I/(j\omega)$. Accordingly, the polarization P can be written as

$$P=\frac{\overline{p}}{a'^3}=\frac{E_0}{j\omega(R+j\omega L)a'}\overline{a_x} \tag{8}$$

based on the electric dipole moment ($\overline{p}=qa'\overline{a_x}$).Through the electric flux density ($\overline{D}=\varepsilon_0 E_0+P$), the effective permittivity can be obtained as

$$\varepsilon_{eff}(\omega)=1+\chi_e(\omega)=1-\frac{\omega_p^2\left(\omega+j\,R/L\right)}{\omega\left[\omega^2+\left(R/L\right)^2\right]} \tag{9}$$

where ε_0 is permittivity in free space, R is total resistance of wire, L is the inductance of wire, χ_e is the electric susceptibility and ω_p is the plasma frequency and the square of it can be written as

$$\omega_p^2=\frac{2\pi}{\mu_0\varepsilon_0 a'^2\ln(a'/r')} \tag{10}.$$

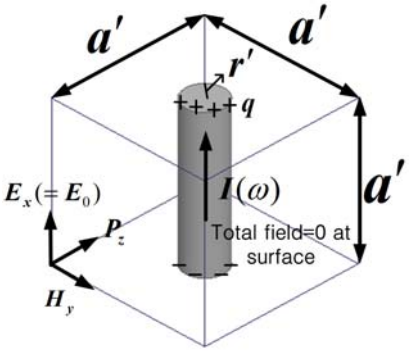

Fig.3. Structure of a thin wire

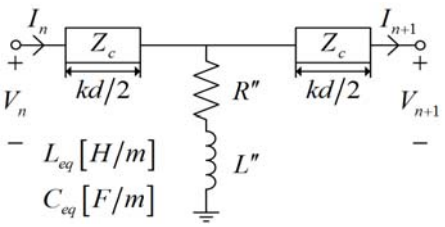

Fig.4. Equivalent circuit for thin wire

An equivalent circuit can be devised very conveniently. By dividing the effective permittivity with the geometrical factor, g, the effective capacitance of a transmission line is given by

$$C_{eff}(\omega) = \frac{\varepsilon_0 \varepsilon_{r,eff}(\omega)}{g} = \frac{\varepsilon_0}{g} - \frac{\omega_p^2}{\omega\left(\omega - j\frac{R}{L}\right)}\varepsilon_0 \cdot \frac{1}{g} \quad \left[F/m\right] \quad (11).$$

Now, the effective shunt admittance can be expressed as

$$Y(\omega) = j\omega C_{eff}(\omega)d = \frac{j\omega\varepsilon_0 d}{g} + \frac{1}{\left(\frac{Rg}{L\omega_p^2\varepsilon_0 d} + j\omega\frac{g}{\omega_p^2\varepsilon_0 d}\right)} (\mho) \quad (12)$$

where d is the physical length of the T/L unit cell. The total shunt admittance of the equivalent circuit in Fig. 4 can be written as

$$Y_{eq}(\omega) = j\omega C_{eq}d + \frac{1}{R'' + j\omega L''}. \quad (13)$$

The values of the parameters R" and L" can be obtained as

$$R'' = Rg(\Omega), \; L'' = Lg(H) \quad (14)$$

by comparing (12) and (13).

IV. VARIFICATION OF MODELINGS AND DISCUSSION

The ring resonator used in the EM simulation is made of copper and is designed at 13.56 MHz. The unit cell size (a) is 12 cm (roughly $0.005\lambda_0$). The radii of the loop (r) and the ring (r_{ring}) are 5 cm and 1 mm, respectively. Let's name this as a standard structure. The ohmic resistance R_l is 0.058 Ω and the radiation loss R_r is negligible at the resonance frequency. The inductance of loop is 266nH. The value of capacitance for the resonance is 533 pF. Fig. 5 (a) and (b) show the extracted [4] real and imaginary part of permeability based on circuit and EM simulations when the TEM wave propagates in the z direction as illustrated in Fig. 1. The circuit parameters based on (7) and (14) are G'=0.0075 mho, C'=40.92 nF, L'=3.37 nH, R''=1 Ω, L''=88.84nH. The loss is the most significant at the resonant frequency of 13.56 MHz as implied by the imaginary part. However, the loss tangent is about 0.05 when the real part of effective permeability crosses -1 at 14 MHz. Fig. 6 (a) and (b) show the real and imaginary part of the effective permittivity for the thin wire when r' and a' are 1mm and 12cm, respectively. The loss tangent is about 0.0011 when the real part of effective permittivity crosses -1 at 347 MHz. The high loss occurs at low frequencies as shown in Fig. 6 (b), but it decreases drastically as the frequency increases. The circuit and EM simulated results show an excellent agreement with the curve (theory) plotted based on (3) and (11), respectively. The excellent agreement validates the proposed modeling. Fig. 7 (a) and (b) show the extracted effective permeability of the ring resonator when the unit cell size, a, and the thickness, r_{ring}, are fixed with 12 cm and 1 mm while the radius, r, varies from 5 cm to 1 cm. The effect of magnetization is seen to decrease

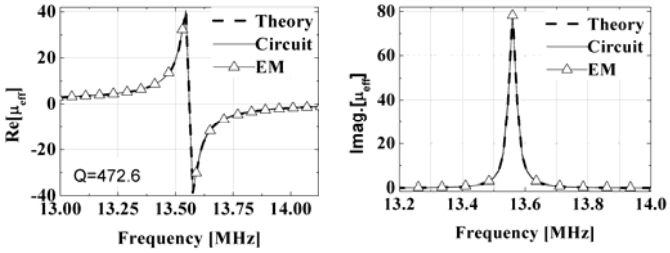

(a) Real (b) Imaginary

Fig. 5. Extracted effective permeability when a=12 cm, r= 5 cm, r_{ring}= 1mm (based on Fig.1)

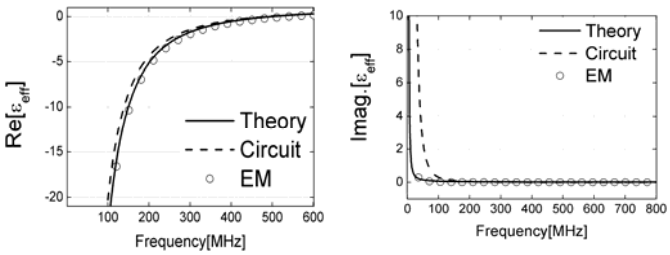

(a) Real (b) Imaginary

Fig. 6. Extracted effective permittivity when a' = 12cm, r' = 1 mm (based on Fig. 3)

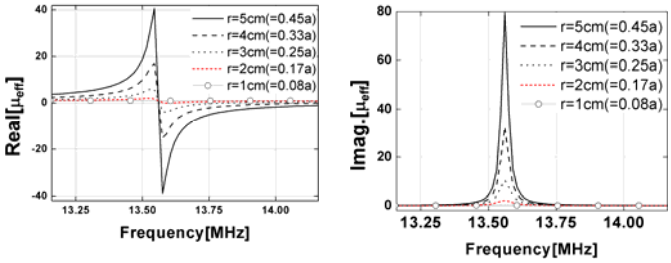

(a) Real (b) Imaginary

Fig. 7. Extracted effective permittivity (a=12cm fixed)

as expected. Fig. 8 and 9 show the real and imaginary part of the effective permeability when the unit cell size (a) varies with respect to the wavelength with the ratio of a, r, and r_{ring} maintained as the standard structure (a=12cm, r=5cm, and r_{ring}=1mm). For this case, r/a and r/r_{ring} (R) are maintained the same. As is expected from (3), the real part of the permeability becomes smoother as the size a decreases. From the imaginary part of the permeability shown, we can see that the loss becomes more significant as a increases near the resonance frequency. On the other hand, at some useful frequencies where μ_{eff}= -1 or μ_{eff}= -2, the loss becomes smaller as a increases. Fig. 10 and 11 show the real and imaginary part of the effective permittivity with respect to the size of unit cell a' and radius r′ of the thin wire. As a' increases, the real part of the effective permittivity is seen to have stiff slopes when they are negative. In the low frequency region, the imaginary part becomes larger as a decreases. However, it is shown to be very close to 0 at higher frequencies.

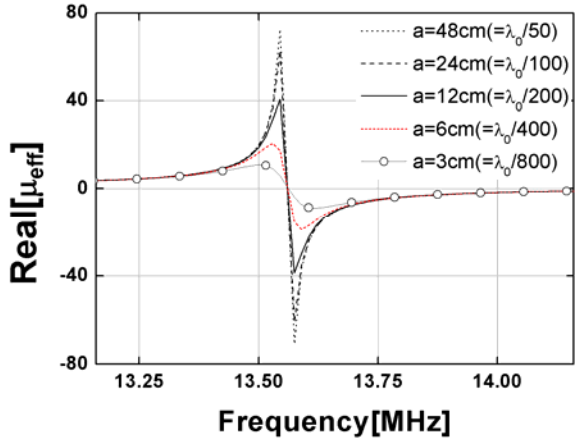

Fig. 8. Real part of μ_{eff} with respect to size of a

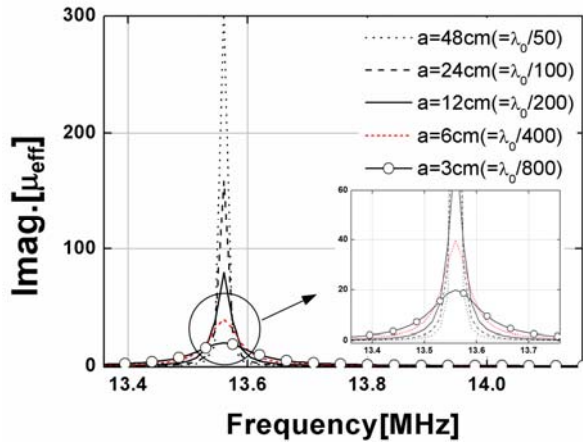

Fig. 9. Imaginary part of μ_{eff} with respect to size of a

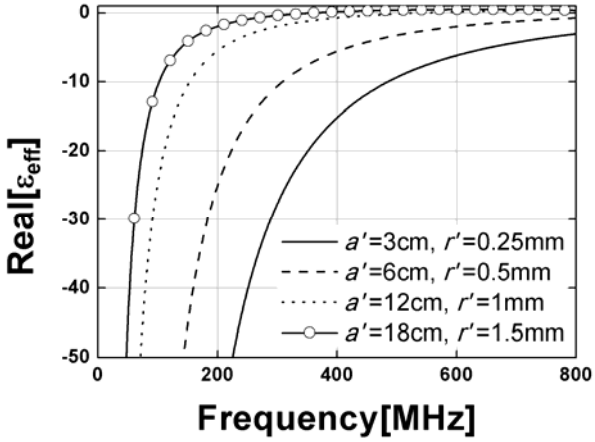

Fig. 10. Real part of ε_{eff} with respect to size of a'

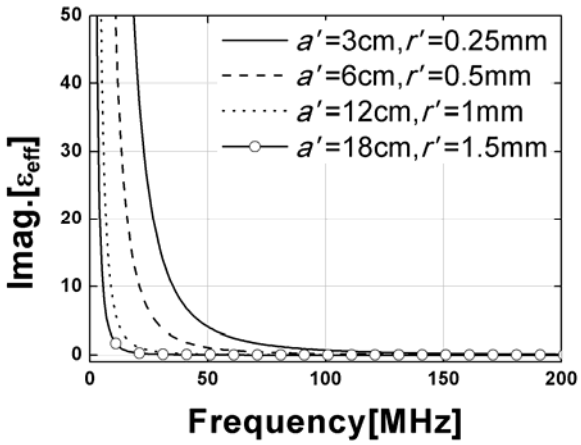

Fig. 11. Imaginary part of ε_{eff} with respect to size of a'

IV. Conclusion

The effective permeability of ring resonators (or SRRs) and the effective permittivity of thin wires have been formulated based on the concept of magnetization and polarization, respectively. Equivalent circuits of them have also been proposed and analyzed with necessary comparisons. The circuit- and EM-simulated results are in excellent agreement. With the provided modeling, the problem of synthesizing the effective medium can be engineered more systematically.

Acknowledgement

This work was supported by Mid-career Researcher Program through the National Research Foundation of Korea (NRF) grant funded by the Korea government (MEST) (No. 2012047938).

References

[1] J.B. Pendry, A.J. Holden, D.J. Robbins, and W. J. Stewart, “Magnetism from conductors and enhanced nonlinear phenomena,” IEEE Transactions on Microwave Theory Technology, vol. 47, pp. 2075–2084, November 1999.

[2] J.B. Pendry, A.J. Holden, D.J. Robbins, and W. J. Stewart, “Low frequency plasmons in thin-wire structures,” Journal of Physics, vol. 10, June 1998.

[3] K. Zhang, Q. Wu, J. Fu, F.Yimeng, and L. Li, “Metamaterials With Tunable Negative Permeability Based on Mie Resonance,”, IEEE Transactions on Magnetics, vol. 48, pp. 4289–4292, November 2012.

[4] S. Mao, S. Chen, C. Huang, "Effective Electromagnetic Parameters of Novel Distributed Left-Handed Microstrip Lines,"IEEE Transactions on Microwave Theory Technology, vol. 53, no. 4, pp. 1515–1521, April, 2005

[5] K. Zhang, Q. Wu, J. Fu, F.Yimeng, and L. Li, “Metamaterials With Tunable Negative Permeability Based on Mie Resonance,”, IEEE Trans. Magnetics, vol. 48, pp. 4289–4292, November 2012

[6] S.M. Rudolph, C. Pfeiffer, and A. Grbic, “Design and Free-Space Measurements of Broadband, Low-Loss Negative-Permeability and Negative-Index Media,”, IEEE Transactions on Antennas and Propagation, vol. 59, pp. 2989–2997, August 2011.